Cardiovascular Research (2012) **93**, 682–693
doi:10.1093/cvr/cvr356

Activated CD47 promotes pulmonary arterial hypertension through targeting caveolin-1

Philip M. Bauer[1,2†], Eileen M. Bauer[2†], Natasha M. Rogers[2], Mingyi Yao[2], Monica Feijoo-Cuaresma[3], Joseph M. Pilewski[4], Hunter C. Champion[2,4], Brian S. Zuckerbraun[1], Maria J. Calzada[3], and Jeffrey S. Isenberg[2,4*]

[1]Department of Surgery, University of Pittsburgh School of Medicine, Pittsburgh, PA, USA; [2]Vascular Medicine Institute, University of Pittsburgh School of Medicine, Pittsburgh, PA, USA; [3]Immunology Service, Instituto de Investigacion Princesa, Department of Medicine, Universidad Autónoma de Madrid, Madrid, Spain; and [4]Division of Pulmonary, Allergy and Critical Care Medicine, University of Pittsburgh School of Medicine, Pittsburgh, PA, USA

Received 14 October 2011; revised 12 December 2011; accepted 22 December 2011; online publish-ahead-of-print 2 January 2012

Time for primary review: 25 days

Aims Pulmonary arterial hypertension (PAH) is a progressive lung disease characterized by pulmonary vasoconstriction and vascular remodelling, leading to increased pulmonary vascular resistance and right heart failure. Loss of nitric oxide (NO) signalling and increased endothelial nitric oxide synthase (eNOS)-derived oxidative stress are central to the pathogenesis of PAH, yet the mechanisms involved remain incompletely determined. In this study, we investigated the role activated CD47 plays in promoting PAH.

Methods and results We report high-level expression of thrombospondin-1 (TSP1) and CD47 in the lungs of human subjects with PAH and increased expression of TSP1 and activated CD47 in experimental models of PAH, a finding matched in hypoxic human and murine pulmonary endothelial cells. In pulmonary endothelial cells CD47 constitutively associates with caveolin-1 (Cav-1). Conversely, in hypoxic animals and cell cultures activation of CD47 by TSP1 disrupts this constitutive interaction, promoting eNOS-dependent superoxide production, oxidative stress, and PAH. Hypoxic TSP1 null mice developed less right ventricular pressure and hypertrophy and markedly less arteriole muscularization compared with wild-type animals. Further, therapeutic blockade of CD47 activation in hypoxic pulmonary artery endothelial cells upregulated Cav-1, increased Cav-1CD47 co-association, decreased eNOS-derived superoxide, and protected animals from developing PAH.

Conclusion Activated CD47 is upregulated in experimental and human PAH and promotes disease by limiting Cav-1 inhibition of dysregulated eNOS.

Keywords Pulmonary arterial hypertension • CD47 • eNOS • Caveolin-1 • Reactive oxygen species

1. Introduction

Pulmonary arterial hypertension (PAH) is a disease of the small pulmonary arteries marked by a progressive increase in pulmonary vascular resistance, leading to uncompensated right heart failure and ultimately death.[1–3] While idiopathic PAH (IPAH) occurs in the absence of any known insult, secondary PAH results from a number of pathological conditions.[4,5] Independent of its aetiology PAH is characterized by remodelling of the pulmonary vasculature, vasoconstriction, and thrombosis *in situ*.[1]

One of the key initiating events leading to PAH is endothelial dysfunction characterized by uncoupling of endothelial nitric oxide synthase (eNOS) and an associated lack of bioavailable nitric oxide (NO).[6–8] Not surprisingly, eNOS null mice are more susceptible to the development of PAH.[9] Regulation of eNOS activity is complex and depends on phosphorylation, protein–protein interactions, and localization to specialized areas of the cell membrane.[10,11] Caveolin-1 (Cav-1) limits eNOS activity via direct association.[12,13] Dissociation or loss of Cav-1 leads to pathological eNOS hyperactivity,[14] and Cav-1 null mice spontaneously develop pulmonary hypertension[15–17] that

† These authors contributed equally to this work.

* Corresponding author. BST, Room E1258, 200 Lothrop Street, University of Pittsburgh School of Medicine, Pittsburgh, PA 15261, USA. Tel: +412 383 5424; fax: +412 648 5980, Email: jsi5@pitt.edu

is ameliorated by re-expression of Cav-1 in the endothelium[18] or eNOS inhibition.[19,20] Finally, in human studies, loss of pulmonary Cav-1 has been linked to PAH.[21,22]

Work by our group has found that the matricellular protein thrombospondin-1 (TSP1), through binding to its cognate receptor CD47, blocks physiological NO responses in vascular cells.[23,24] Pulmonary vascular endothelial cells from TSP1 and CD47 null mice maintain elevated levels of the NO second messenger cyclic guanosine monophosphate (cGMP).[25,26] Recent data also indicate that plasma TSP1 is a potent inhibitor of eNOS in endothelium and suppresses endogenous NO production in the vasculature.[27]

We hypothesized that TSP1 and CD47 contribute to the development of PAH in humans. Interestingly, we observed a marked upregulation of TSP1 and CD47 protein and mRNA in patients with PAH. Findings of upregulation of the TSP1-CD47 axis in human PAH were paralleled by upregulation of both TSP1 and CD47 in experimental models of PAH. In pulmonary endothelial cells, CD47 constitutively associates with Cav-1. Conversely, in hypoxic animals and cell cultures, activation of CD47 by TSP1 disrupts this constitutive interaction, promoting eNOS-dependent superoxide production, oxidative stress, and PAH. Hypoxic TSP1 null mice developed less right ventricular pressure and hypertrophy and markedly less arteriole muscularization and thickening compared with wild-type animals. Therapeutic blockade of CD47 activation in hypoxic pulmonary arterial endothelial cells upregulated Cav-1, increased Cav-1CD47 co-association, decreased eNOS-derived superoxide, and protected animals from developing PAH.

2. Methods

Detailed information on the materials and methods used in this study is provided in the Supplementary material online.

2.1 Animal studies

All studies were performed under a protocol approved by the University of Pittsburgh Institutional Animal Care and Use Committee (IACUC) or under a protocol approved by the Committee for Research and Ethics of the Universidad Autonoma de Madrid and in accordance with Directive 2010/63/EU of the European Parliament. Male C57BL/6 wild-type, TSP1, and CD47 null mice (stock numbers 000664, 006141, and 003173, respectively) were obtained from the Jackson Laboratory (Bar Harbor, ME, USA). Male Sprague Dawley rats were obtained from Harlan (Indianapolis, IN, USA). Adequacy of anaesthesia was monitored at all times by assessment of skeletal muscle tone, respiration rate and rhythm, and response to tail pinch. Euthanasia was achieved by isoflurane inhalational anaesthesia (1.5%) and concurrent cervical dislocation (mice) or anaesthetic overdose (rats) as approved by the respective University IACUCs.

2.2 Human tissue studies

Use of human tissues was within ongoing IRB approved protocols at the University of Pittsburgh and Johns Hopkins University and conformed to the principles outlined in the Declaration of Helsinki.

2.3 Cell cultures

Primary murine pulmonary microvascular endothelial cells were harvested from 8- to 10-week-old male C57BL/6 wild-type and TSP1 null mice as previously published.[26] Human pulmonary arterial and microvascular endothelial cells were purchased from Lonza (Switzerland).

2.4 Murine chronic hypoxic exposure model of PAH

Nine- to 12-week-old male wild-type, TSP1 and CD47 null mice were placed in an airtight hypoxia chamber and exposed to acute (FiO_2= 7.5%) or chronic (FiO_2= 10%) hypoxia for the indicated time. Mice maintained in room air served as controls.

2.5 Haemodynamic and ventricular weight measurements

Animals were anaesthetized with pentobarbital (40 mg/kg ip). The trachea was cannulated, and animals were ventilated with 1.5% isoflurane. The thoracic cavity was opened, a Millar catheter was inserted into the right ventricle (RV), and RV systolic pressure was measured with PowerLab monitoring equipment. The ratio of RV weight to left ventricular (LV) weight plus septum (S) (RV/LV + S) was used as an index of RV hypertrophy (Fulton Index).

2.6 Murine lung histology

Mouse lungs were perfused with PBS, fixed with 4% paraformaldehyde under a standardized inflation pressure and excised (12 h PFA 4°C). Lungs were transferred into 30% sucrose (overnight, 4°C), paraffin embedded and sectioned (10 μm), and stained for α-smooth muscle actin. For pulmonary vascular morphometry studies, images of peripheral arterioles were captured with a Nikon Eclipse 800 microscope.

2.7 Rat monocrotaline model of PAH

As we have previously published, male Sprague Dawley rats were treated with monocrotaline (50 mg/kg)[28] or monocrotaline and a CD47-blocking antibody (clone OX101, 1 μg/gram body weight) on day 1 and day 14. On day 28, animals were anaesthetized with pentobarbital (40 mg/kg ip) and 2% isoflurane and right RV pressure and Fulton index determined. Lung sections were stained with haematoxylin and eosin. Images for arterioles were captured with a microscope digital camera system (Provus, Olympus), and arterial area was measured using an image analysis programme.

2.8 Protein expression by western blot analysis

Lysates of lung tissues (human, murine, and rat) and human and murine pulmonary endothelial cells were subjected to western analysis. Protein was resolved by SDS–PAGE and transferred onto nitrocellulose. Blots were probed with primary antibody to the respective proteins and were visualized after 1 h incubation in secondary antibody on an Odyssey Imaging System (Licor).

2.9 Co-immunoprecipitation

Immunoprecipitation was performed as we have published with minor modification.[27] Human pulmonary microvascular endothelial cells (passages 2–4) were serum starved over 24 h, incubated in basal medium without serum containing 0.1% BSA for 90 min and then treated with TSP1 ± hypoxia (1% O_2) for 4 h, lysate prepared and precipitated with a Cav-1 or a CD47 antibody. Protein was separated via gel electrophoresis and transferred to membranes and blotted against Cav-1 or CD47.

2.10 siRNA knockdown of Cav-1

All siRNAs were designed and synthesized by Dharmacon (ThermoFisher Scientific). siRNA transfection was performed using a lipofectamine reagent (Invitrogen) according to the manufacturer's instructions. Gene silencing was established by western blot analysis 72 h after transfection.

2.11 Real-time quantitative PCR

Total RNA from murine and human samples was extracted using Qiagen RNeasy® Mini Kits (Qiagen). One microgram of RNA was

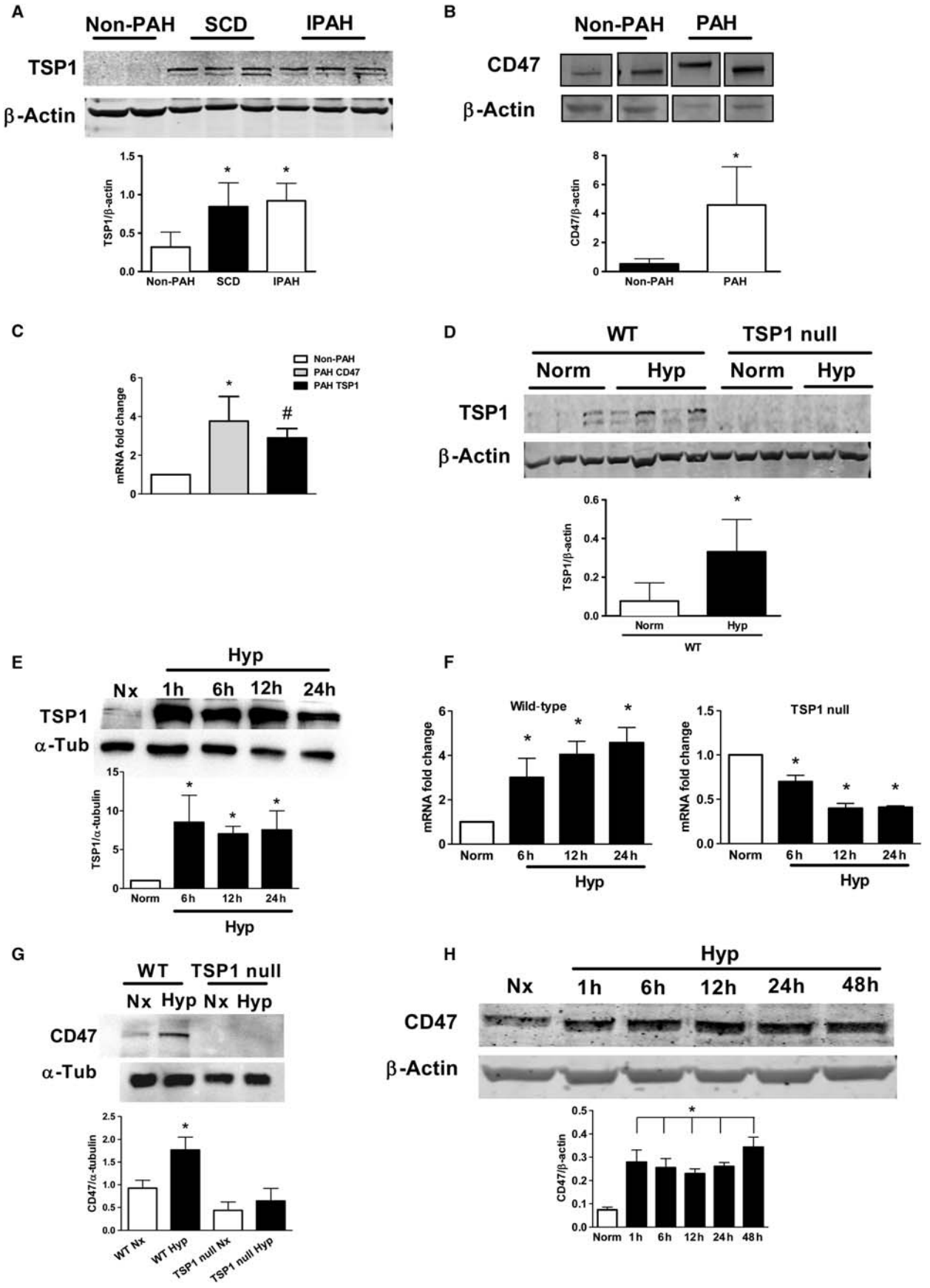
A
Non-PAH
SCD
IPAH
TSP1
β-Actin
TSP1/β-actin
Non-PAH
SCD
IPAH
B
Non-PAH
PAH
CD47
β-Actin
CD47/β-actin
Non-PAH
PAH
C
Non-PAH
PAH CD47
PAH TSP1
mRNA fold change
D
WT
TSP1 null
Norm
Hyp
Norm
Hyp
TSP1
β-Actin
TSP1/β-actin
Norm
Hyp
WT
E
Hyp
Nx
1h
6h
12h
24h
TSP1
α-Tub
TSP1/α-tubulin
Norm
6h
12h
24h
Hyp
F
Wild-type
TSP1 null
mRNA fold change
Norm
6h
12h
24h
Hyp
G
WT
TSP1 null
Nx
Hyp
Nx
Hyp
CD47
α-Tub
CD47/α-tubulin
WT Nx
WT Hyp
TSP1 null Nx
TSP1 null Hyp
H
Hyp
Nx
1h
6h
12h
24h
48h
CD47
β-Actin
CD47/β-actin
Norm
1h
6h
12h
24h
48h

treated with DNase I (Invitrogen) and then reverse-transcribed. cDNA was amplified using Platinum® PCR SuperMix-UDG (Invitrogen). For details on primers and cycle conditions, see the supplementary material online.

2.12 Determination of monomer to dimer ratio eNOS protein

Tissue samples were prepared as described for western analysis with the following exceptions: samples of equal protein content were kept for 5 min at room temperature and one sample was boiled to serve as a control for monomer formation. Samples were then resolved on an 8% SDS–PAGE on ice, at 100 V and transferred and blotted against total eNOS.

2.13 Determination of nitrotyrosine formation in the lung

Lung sections were de-paraffinized, rehydrated, and microwaved in sodium citrate buffer (pH 6, 10 min) for antigen retrieval. Sections were blocked and stained with a rabbit nitrotyrosine antibody (rabbit anti-nitrotyrosine, Millipore, 1 : 100, Cat. No. ab5411) in combination with a Vectastain ABC kit (Vector Laboratories) and a metal-enhanced DAB substrate kit (Thermo Scientific). Sections were counterstained for haematoxylin (Vector Laboratories), dehydrated, and covered.

2.14 Measurement of intracellular O_2^-

Human pulmonary artery endothelial cells (hPAEC) were grown to confluence and exposed to 1% O_2 or normoxia for 24 h. Dihydroethidium (DHE) was added for the final 30 min of the 24 h incubation period. O_2^- was evaluated by measuring the conversion of DHE to hydroxyethidium in a fluorimeter.

2.15 Gain-of-function studies in pulmonary endothelial cells

Murine pulmonary endothelial cells were harvested from age-matched male wild-type and TSP1 null mice. Cells were plated at 80% confluence, treated with normoxia or hypoxia (1% O_2) ± exogenous TSP1 for 24 h, cell lysate prepared and western blot analysis performed.

2.16 Statistics

Statistics were performed using GraphPad Prism software (GraphPad Software, Inc., CA, USA). Data were analysed by one-way ANOVA followed by the Tukey test for multiple comparisons. For grouped analysis, data were analysed by two-way ANOVA followed by the Bonferroni post hoc test.

3. Results

3.1 TSP1 and its cognate receptor CD47 are increased in PAH

The role of TSP1 in clinical PAH is unknown. *Figure 1A* shows a representative western blot of lung specimens from a historical cohort of non-PAH patients, scleroderma-associated PAH patients (SCD), and patients with IPAH. Densitometry of western blots from the total cohort of 10 non-PAH patients, and 10 PAH patients (five SCD and five IPAH), reveals a significant increase in TSP1 protein expression in both SCD and IPAH compared with samples from patients without PAH ($P < 0.05$). Equally unknown is the role of CD47 in PAH. Western blot analysis of lung samples from a prospective cohort (three control and five PAH patients) demonstrated upregulation of pulmonary CD47 (*Figure 1B*) and TSP1 (data not shown) in PAH lungs compared with control lungs. Analysis of transcript demonstrated a significant fold increase in both TSP1 and CD47 mRNA in PAH samples (*Figure 1C*).

3.2 Activated CD47 and TSP1 are upregulated in hypoxic murine PAH

Chronic hypoxia is an established method of inducing experimental PAH[29] and has a role in disease pathogenesis in human subjects.[30–32]

Figure 1 Pulmonary TSP1 and CD47 are upregulated in human subjects with PAH and in experimental PAH. (*A*) Lung tissue from a historical cohort of non-PAH, IPAH or SCD was probed by western blot for TSP1 and β-actin. (western blot is the only representative). Densitometry is the result of 10 non-PAH patients, five SCD, 5 IPAH patients and is presented as mean ratio of TSP1 to β-actin (± SD). Asterisk (*) indicates statistically significant difference ($P < 0.05$) compared with non-PAH patients. (*B*) Western blot analysis of lung samples from a prospective cohort of non-PAH and PAH patients probed for CD47 and β-actin. Densitometry is the result of three non-PAH and five PAH patients. Asterisk (*) indicates statistically significant difference ($P < 0.05$) compared with non-PAH patients. (*C*) TSP1 and CD47 mRNA expression levels in lung samples from the prospective cohort. Representative data from three independent experiments are presented. mRNA levels are expressed as fold change over non-PAH and normalized with 18S ribosomal subunit levels as endogenous non-PAH. Asterisk (*) indicates statistically significant difference ($P < 0.05$) compared with control. Hash (#) indicates statistically significant difference ($P < 0.05$) compared with non-PAH. (*D*) Representative western blot of lung tissue from normoxic and chronically hypoxic (21 days normobaric 10% O_2) C57BL/6 wild-type and TSP1 null mice probed against TSP1 and β-actin. Densitometry is presented as mean ratio of TSP1 to β-actin (± SD). Asterisk (*) indicates statistically significant difference ($P < 0.05$) compared with normoxic mice and is based on an analysis of eight mice per group. (*E*) Representative western blot probed against TSP1 and α-tubulin from lung samples from normoxic and acute hypoxia (normobaric 7.5% O_2) challenged wild-type mice. Representative data from three independent experiments are presented. Densitometry is presented as mean ratio of TSP1 to α-tubulin (± SD). Asterisk (*) indicates statistically significant difference ($P < 0.05$) compared to normoxia and is based on four mice at each time point. (*F*) TSP1 mRNA expression levels in lung samples from wild-type and TSP1 null mice exposed to normoxia or hypoxia (normobaric 7.5% O_2) for the indicated time points. Representative data from three independent experiments are presented. mRNA levels are expressed as fold change over normoxic conditions and normalized with HPRT levels as endogenous control. Asterisk (*) indicates statistically significant difference ($P < 0.05$) compared with normoxia. (*G*) Representative western blot of wild-type and TSP1 null pulmonary microvascular endothelial cells exposed to normoxia or hypoxia (normobaric 1% O_2) for 12 h probed against CD47 and α-tubulin. Representative data from three independent experiments are presented. Densitometry is presented as mean ratio of CD47 to α-tubulin (± SD). Asterisk (*) indicates statistically significant difference ($P < 0.05$) compared with normoxia. (*H*) Representative western blot from wild-type mice exposed to acute hypoxia for the indicated time points probed against CD47 and β-actin. Densitometry from analysis of western results from four mice in each treatment group is presented as mean ratio of CD47 to β-actin (± SD). Asterisk (*) indicates statistically significant difference ($P < 0.05$) compared with normoxia.

We wished to determine whether TSP1 and CD47 were also induced in experimental PAH. Chronically hypoxic wild-type mice demonstrated significantly increased pulmonary TSP1 expression compared with normoxic controls (*Figure 1D*). Wild-type mice exposed to acute hypoxia demonstrated rapid induction of pulmonary TSP1 expression within 1 h (*Figure 1E*) that was paralleled by increases in TSP1 mRNA in lungs from wild-type mice (*Figure 1F*). TSP1 null mice have only partial deletion of the thrombospondin-1 (*THBS1*) gene and residual TSP1 mRNA transcript can be detected on PCR, but functional protein is not detectable on western.[33] TSP1 null mice did not show pulmonary expression of TSP1 protein under normoxoia or hypoxia (*Figure 1D*). However, in TSP1, null mice acute hypoxia decreased pulmonary TSP1 mRNA transcript (*Figure 1F*). In wild-type murine pulmonary microvascular endothelial cells, hypoxia induced expression of CD47 (*Figure 1G*). Interestingly, in normoxic TSP1 null pulmonary endothelial cells, CD47 expression was significantly lower compared with wild-type cells with no increase under hypoxia (*Figure 1G*). Analysis of lungs from hypoxic wild-type mice also demonstrated rapid induction of pulmonary CD47 (*Figure 1H*).

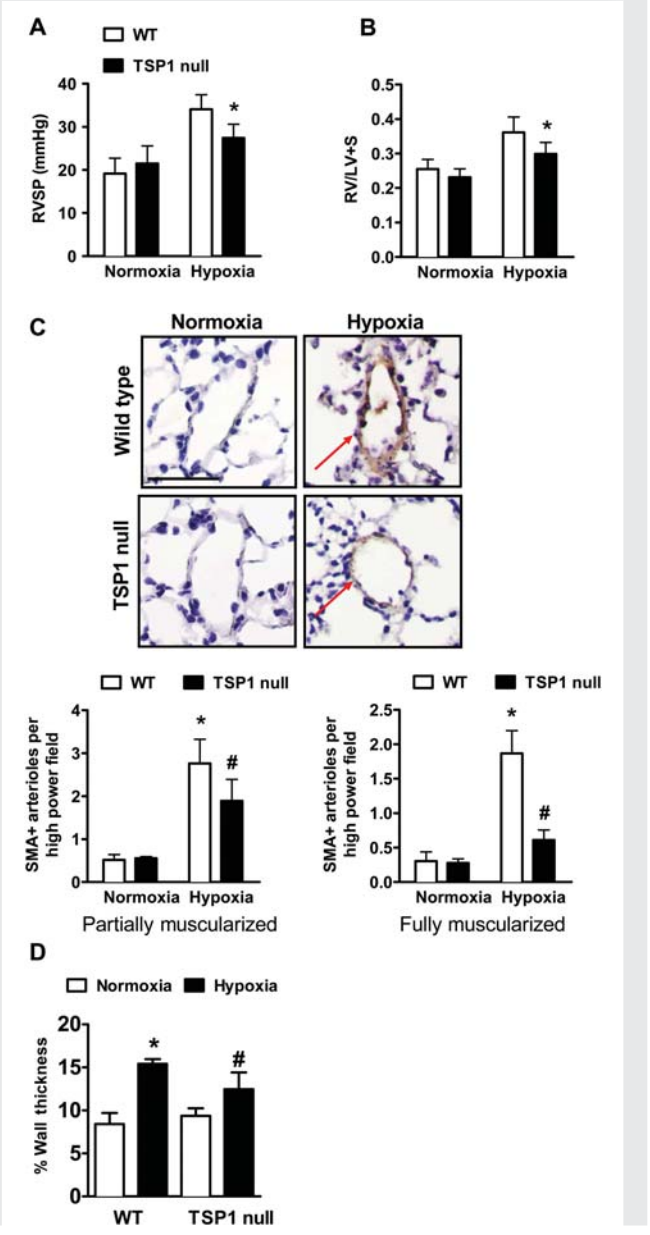

3.3 Activation of CD47 by TSP1 promotes hypoxic PAH

In experimental PAH and human disease, increased pulmonary vascular resistance results in increased right ventricular (RV) pressure and secondary RV hypertrophy.[34] Chronic hypoxia led to a significant rise in RV pressure with associated RV hypertrophy in wild-type mice. However, in the absence of activated CD47, as in the TSP1 null mice, chronic hypoxia resulted in significantly decreased RV pressure and RV hypertrophy compared with wild-type animals (*Figure 2A* and *B*).

A hallmark of PAH is vascular remodelling.[3] *Figure 2C* shows representative images of pulmonary arterioles from each treatment group stained for α-smooth muscle actin (brown staining). In the absence of CD47 activation, hypoxic TSP1 null mice demonstrated significantly fewer partially and fully muscularized arterioles in lung tissue sections compared with lung sections from wild-type mice. Results obtained by immunohistology were confirmed by analysis of arteriole wall thickness. Sections of lungs from hypoxic TSP1 null mice demonstrated significantly less wall thickening compared with lung sections from hypoxic wild-type mice (*Figure 2D*).

3.4 Under hypoxia activated CD47 inhibits upregulation of Cav-1

Next, we tested if activated CD47 promotes PAH through the inhibition of eNOS. Hypoxic wild-type and TSP1 null mice demonstrated increased pulmonary eNOS protein expression (*Figure 3A* and *B*). Maximal eNOS activity is associated with phosphorylation of eNOS at serine^{1176} in mice.[35] Hypoxic wild-type mice showed no change in the ratio of phospho-eNOS to total eNOS compared with wild-type normoxic mice (*Figure 3A* and *C*). Normoxic TSP1 null mice demonstrated increased pulmonary eNOS phosphorylation of

Figure 2 Activated CD47 promotes hypoxia-stimulated PAH. Wild-type and TSP1 null mice were exposed to 21 days chronic hypoxia (normobaric 10% O_2) or room air. At the end of the exposure period, (*A*) right ventricular systolic pressure (RVSP), and (*B*) right ventricular hypertrophy (Fulton Index, RV/LV + S) were determined. Data represent mean ± SD ($n = 8$ per group). Asterisk (*) indicates statistically significant difference ($P < 0.05$) compared with hypoxic wild-type. (*C*) Representative images of pulmonary tissue sections from normoxic and hypoxic male C57BL/6 wild-type and TSP1 null mice demonstrating pulmonary arterioles stained for α-smooth muscle actin (red arrows). Scale bar represents 50 μm. Sections of lungs were analysed for partial and full muscularization of arterioles by an observer blinded to strain and treatment. Quantification was based on 20 random 40x fields per section and three sections per mouse. $n = 8$ mice per group, analysis is the result of 10 vessels per section. Asterisk (*) indicates statistically significant difference ($P < 0.05$) compared with normoxic wild-type. Hash (#) indicates statistically significant difference ($P < 0.05$) compared with hypoxic wild-type. (*D*) Quantification of arteriole wall thickness of lung sections by a blinded observer based on 20 random 40x fields per section. Asterisk (*) indicates statistically significant difference ($P < 0.05$) compared with normoxic wild-type. Hash (#) indicates statistically significant difference ($P < 0.05$) compared with hypoxic wild-type.

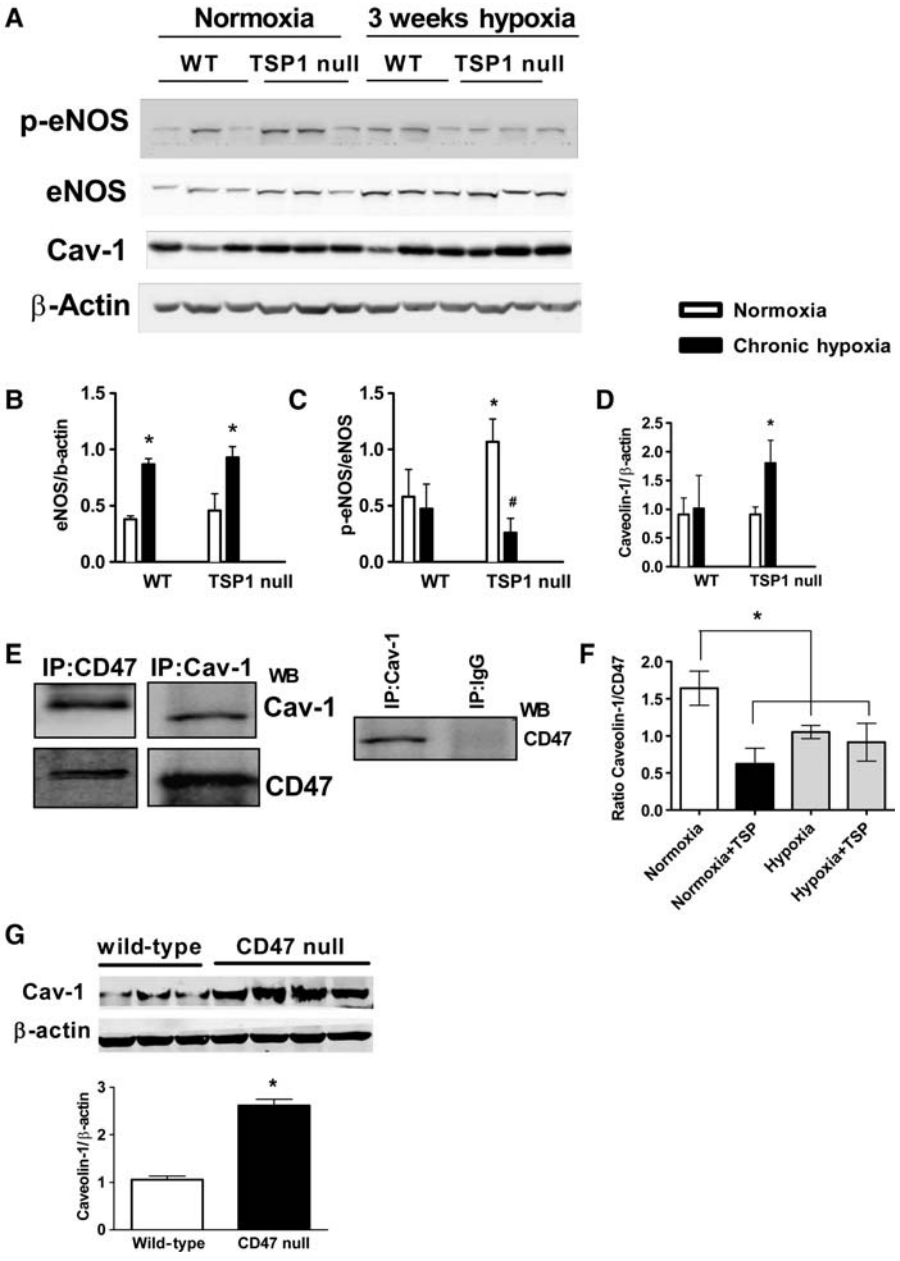

Figure 3 Activated CD47 regulates hypoxic eNOS by altering Cav-1CD47 co-association. (*A*) Western blot of lung tissue from wild-type and TSP1 null mice exposed to chronic hypoxia or room air probed against total eNOS protein, eNOS phosphorylation at serine-1176 (murine residue), Cav-1, and β-actin. Quantification of densitometric analysis of the ratio of (*B*) total eNOS to β-actin, (*C*) p-eNOS to total eNOS, (*D*) Cav-1 to β-actin. Asterisk (*) indicates statistically significant difference ($P < 0.05$) compared with wild-type normoxic. Hash (#) indicates statistically significant difference ($P < 0.05$) compared with wild-type normoxic. All ratios represent mean ± SD and are the result of the total cohort ($n = 8$ animals per group). (*E*) Co-immunoprecipitation in human pulmonary microvascular endothelial cells of Cav-1 and CD47. Immunoprecipitation was with monoclonal antibodies to Cav-1, CD47, or an isotype-matched control IgG antibody. Results presented are representative of four separate experiments. (*F*) Human pulmonary microvascular endothelial cells were serum starved and then treated with TSP1 (2.2 nmol/L) ± hypoxia (1% O_2 for 4 h), lysate prepared and immunoprecipitation for CD47 performed with protein blotted for Cav-1. Results are presented as the quantification of densitometric analysis from three separate experiments of the ratio of Cav-1 to CD47 following immunoprecipitation. Asterisk (*) indicates statistically significant difference ($P < 0.05$) compared with normoxia. (*G*) Western blot of pulmonary Cav-1 from lung lysate from chronically hypoxic (21 days normobaric 10% O_2) wild-type ($n = 3$) and CD47 null ($n = 4$) mice. Asterisk (*) indicates statistically significant difference ($P < 0.05$) compared with wild-type.

serine[1176] (*Figure 3A* and *C*). However, hypoxic TSP1 null mice displayed a decrease in pulmonary eNOS activity (phosphorylation) compared with normoxic null mice (*Figure 3A* and *C*) indicating that under hypoxia, CD47 does not directly inhibit eNOS activation.

These results raised the possibility that CD47 promotes PAH through alternative mechanisms. We examined Cav-1 expression in our hypoxic mice. Interestingly, in the lungs of hypoxic TSP1 null mice, and therefore absent activated CD47, Cav-1 was significantly upregulated (*Figure 3A* and *D*). By contrast, in the lungs of hypoxic wild-type mice, and therefore with activated CD47, no upregulation of Cav-1 was observed.

3.5 Cav-1 and CD47 co-associate on pulmonary endothelial cells and both TSP1 and hypoxia decrease this interaction

To account for the increased pulmonary Cav-1 in TSP1 null mice, we hypothesized that CD47 may interact with Cav-1. In lysates from human pulmonary microvascular endothelial cells, Cav-1 was co-precipitated by a CD47 monoclonal antibody and, conversely, CD47 was co-precipitated by a Cav-1 monoclonal antibody (*Figure 3E*). An isotype-matched control IgG antibody did not co-precipitate Cav-1 (*Figure 3E*) or CD47 (data not shown). Treating normoxic pulmonary endothelial cells with TSP1 decreased Cav-1-CD47 association (*Figure 3F*). Hypoxia, through upregulation of TSP1 (see *Figure 5*), decreased Cav-1CD47 association and exogenous TSP1 did not decrease this further (*Figure 3F*). Finally, lung samples from hypoxic CD47 null mice demonstrated increased Cav-1 expression compared with hypoxic wild-type animals (*Figure 3G*).

3.6 Activated CD47 promotes ROS in experimental PAH

PAH in Cav-1 null mice is mediated through overactive uncoupled eNOS and eNOS-derived reactive oxygen species (ROS).[15–17] This suggested upregulation of Cav-1 in hypoxic TSP1 null mice may be a protective mechanism to suppress ROS production from dysregulated eNOS. To test if eNOS is dysregulated in our murine model of PAH, we determined eNOS monomer to dimer ratio (an established marker of eNOS enzymatic uncoupling and dysregulation)[36,37] in pulmonary samples from hypoxic mice. Hypoxic wild-type and TSP1 null lungs showed a comparable increase in eNOS monomer to dimer ratio (*Figure 4A* and *B*).

We predicted that because pathological eNOS uncoupling occurred to an equal degree in lungs from both hypoxic wild-type and TSP1 null mice that this would result in comparable amounts of eNOS-derived ROS, oxidative stress, and protein nitration in both groups. Immunostaining of lung sections revealed increased nitrotyrosine staining in the samples from hypoxic wild-type mice. Surprisingly, hypoxic TSP1 null mice that lack activated CD47 demonstrated minimal nitrotyrosine staining of lung tissues (*Figure 4C*).

3.7 Activated CD47 promotes hypoxia-mediated ROS by inhibiting Cav-1

We next determined whether hypoxia-induced ROS production in hPAEC was associated with upregulation of TSP1. Exposure of hPAEC to hypoxia resulted in increased TSP1 expression (*Figure 5A* and *B*). This correlated with increased production of superoxide

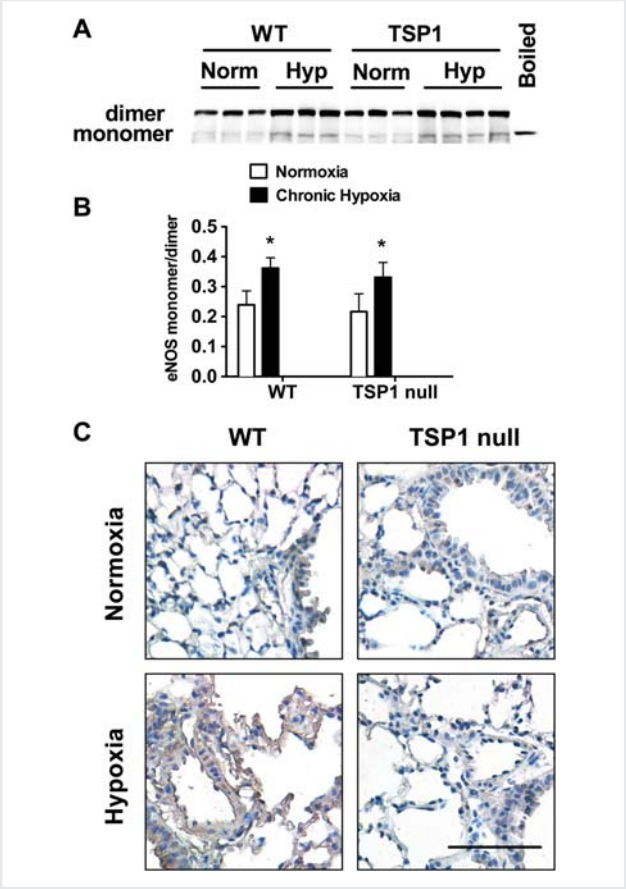

Figure 4 Activated CD47 promotes oxidative stress in hypoxic PAH. (*A*) Representative native gel electrophoresis of lung lysates probed against eNOS to determine eNOS monomer to dimer ratio in lung lysates from wild-type and TSP1 null mice after chronic hypoxia or room air. (*B*) Densitometry is presented as monomer to dimer ratio of eNOS expression and are presented as the mean ± SD ($n = 4$). Asterisk (*) indicates statistically significant difference ($P < 0.05$) compared with normoxic control. (*C*) Representative photomicrographs of lung tissue from wild-type and TSP1 null mice exposed to chronic hypoxia or normoxia stained using an antibody against 3-nitrotyrosine. Immunohistochemistry was performed on two sections from four mice in each group. Scale bar represents 100 μm.

(*Figure 5D*) that was completely abrogated by the eNOS inhibitor L-NAME (*Figure 5D*), identifying uncoupled eNOS activity as the source of the ROS. To determine whether the increased eNOS-derived superoxide occurred via activation of CD47, we treated hPAEC with a CD47 activation blocking antibody.[38] Treating hPAEC with the CD47 antibody inhibited hypoxia-induced superoxide production (*Figure 5D*), while increasing Cav-1 expression (*Figure 5A* and *C*).

To provide further proof that Cav-1 plays a role in ROS production by activated CD47, we used siRNA to knockdown Cav-1. Treatment of hPAEC with Cav-1 siRNA resulted in ~90% decrease in Cav-1 expression (*Figure 5E*). Exposure of control siRNA-treated cells to hypoxia had no effect on superoxide production or the ability of the CD47-blocking antibody to inhibit superoxide production (*Figure 5F*). However, knockdown of Cav-1 resulted in an increase

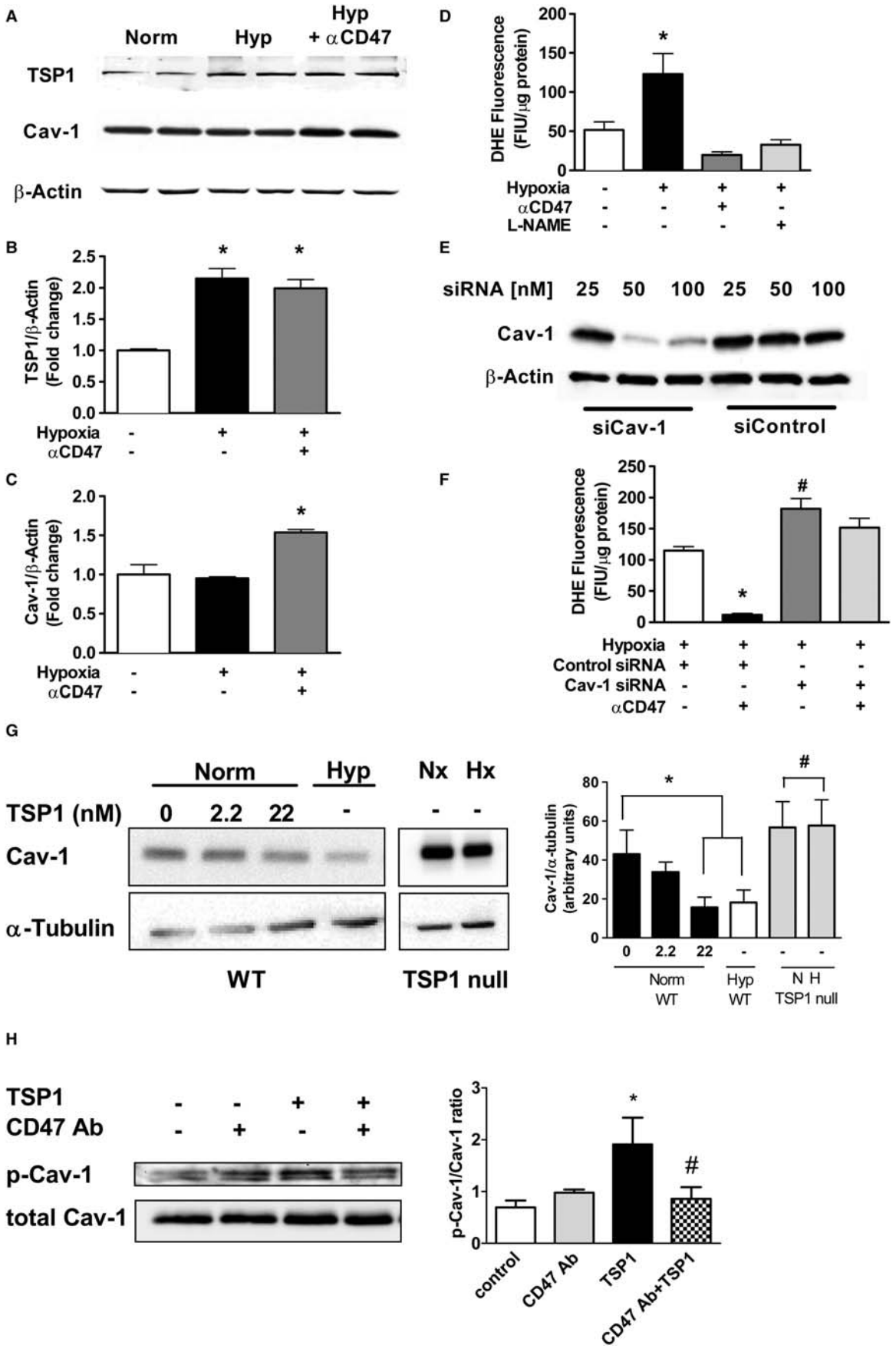
A
Norm
Hyp
Hyp + αCD47
TSP1
Cav-1
β-Actin
B
TSP1/β-Actin (Fold change)
Hypoxia
αCD47
C
Cav-1/β-Actin (Fold change)
Hypoxia
αCD47
D
DHE Fluorescence (FIU/μg protein)
Hypoxia
αCD47
L-NAME
E
siRNA [nM] 25 50 100 25 50 100
Cav-1
β-Actin
siCav-1
siControl
F
DHE Fluorescence (FIU/μg protein)
Hypoxia
Control siRNA
Cav-1 siRNA
αCD47
G
Norm
Hyp
Nx Hx
TSP1 (nM) 0 2.2 22 - - -
Cav-1
α-Tubulin
WT
TSP1 null
Cav-1/α-tubulin (arbitrary units)
0 2.2 22 - - -
Norm WT
Hyp WT
N H TSP1 null
H
TSP1
CD47 Ab
p-Cav-1
total Cav-1
p-Cav-1/Cav-1 ratio
control
CD47 Ab
TSP1
CD47 Ab+TSP1

in hypoxia-induced superoxide and abolished the ability of the CD47 antibody to inhibit superoxide production. In gain-of-function experiments treating murine wild-type pulmonary microvascular endothelial cells with TSP1 to activate CD47 inhibited Cav-1 expression in a dose-dependent manner (*Figure 5G*), as did hypoxia. Conversely, Cav-1 was significantly upregulated under normoxia and hypoxia in TSP1 null pulmonary endothelial cells (*Figure 5G*). Cav-1 phosphorylation has been linked to eNOS activity.[39] Treating hPAEC with TSP1 increased phosphorylation of Cav-1 at Tyr14, whereas pre-treating with a CD47-blocking antibody inhibited TSP1-mediated Cav-1 phosphorylation (*Figure 5H*).

3.8 CD47 is activated in a monocrotaline model of PAH

Monocrotaline-induced PAH is associated with dysregulated uncoupled eNOS,[40] decreased Cav-1 expression,[41] and increased pulmonary ROS production.[42] In rats treated with monocrotaline pulmonary TSP1 and CD47 were upregulated (*Figure 6A* and *B*) and Cav-1 expression decreased (*Figure 6E*). Pulmonary eNOS activity was modestly decreased in monocrotaline-treated animals but was enhanced in animals treated with a rat-specific CD47-blocking antibody (*Figure 6C*).

3.9 Blocking CD47 activation suppresses pulmonary TSP1, upregulates Cav-1, and abrogates monocrotaline-induced PAH

Next, we tested if a CD47-blocking antibody could prevent monocrotaline-induced PAH. Animals received a CD47 antibody[43] at the time of monocrotaline treatment and 14 days later. Control animals demonstrated increased RV systolic pressure and RV hypertrophy 4 weeks after monocrotaline treatment. In contrast, animals treated with a CD47 antibody demonstrated no significant elevation in RV systolic pressure or RV hypertrophy, as defined by Fulton Index (RV/LV + S), and minimal arteriole wall thickening in pulmonary tissue sections (*Figure 6D*). These protective effects were accompanied by both downregulation of pulmonary TSP1 (*Figure 6A*) and upregulation of pulmonary Cav-1 (*Figure 6E*).

4. Discussion

TSP1 has not previously been linked to clinical PAH. We now show that TSP1 protein and transcript are elevated in human PAH. Similarly, in two experimental models of PAH, we observed induction of pulmonary TSP1. CD47 was also upregulated in both clinical and experimental PAH and hypoxic pulmonary endothelial cells. TSP1 null pulmonary endothelial cells expressed significantly less CD47 compared with wild-type cells, and were resistant to hypoxic induction of CD47. These data suggest that TSP1 may also function to regulate CD47. Further, results herein identify CD47 as a proximate promoter of PAH. In the absence of CD47 activation, TSP1 null mice are protected from hypoxia-induced PAH. Compared with wild-type mice, TSP1 null animals displayed reduced RV systolic pressure and RV hypertrophy (by Fulton Index). Histological assessment of null lung sections showed fewer partial and fully muscularized pulmonary arterioles and less arteriole thickening. Also antibody blockade of CD47 activation in a rat model of PAH resulted in near-normal RV pressure and size, and minimal arteriole thickening.

Under hypoxic conditions, and in PAH, activated CD47 suppresses Cav-1 allowing uncoupled eNOS to produce pathological ROS. Conversely, hypoxic TSP1 null pulmonary endothelial cells and null mice, both lacking activated CD47, displayed significantly increased Cav-1 and decreased pathological ROS. That eNOS is the source of this pathological ROS is supported by the finding that ROS production was L-NAME inhibitable. Alternatively, suppression of Cav-1 has been linked to upregulation of NAPDH-oxidase-dependent ROS suggesting an additional mechanism that, in part, may account for pathological ROS in our experiments.[44] Though results in cell and animal studies demonstrate a clear link between CD47 activation and increased pulmonary ROS, it is not clear if this occurred concurrently with a decrease in bioavailable NO.

Post-translation control of eNOS occurs through a number of mechanisms including acetylation,[45] calcium regulation,[46] phosphorylation of key protein residues,[47] and protein–protein interactions.[10] Normoxic TSP1 null mice displayed increased activation of pulmonary eNOS (defined as increased serine^{1176} phosphorylation). These

Figure 5 Blocking CD47 activation upregulates Cav-1 to inhibit eNOS-derived superoxide production in hypoxic pulmonary arterial endothelial cells. (*A*) Representative western blot of hPAEC exposed to normoxia, hypoxia (1% O_2 for 12 h), or hypoxia plus a CD47-blocking antibody (αCD47, clone B6H12, 1 μg/mL). Quantification of densitometric analysis of the ratio of (*B*) TSP1 to β-actin and (*C*) Cav-1 to β-actin. Asterisk (*) indicates statistically significant difference ($P < 0.05$) from normoxic control. (*D*) Superoxide production in hPAEC exposed to normoxia, hypoxia (1% O_2 for 12 h), hypoxia plus L-NAME (100 mmol/L), or hypoxia plus a CD47-blocking antibody (clone B6H12, 1 μg/mL). Asterisk (*) indicates statistically significant difference ($P < 0.05$) from normoxic control. (*E*) Western blot analysis for Cav-1 expression in hPAEC transfected with control or Cav-1 siRNA. (*F*) Superoxide production in hPAEC transfected with control or Cav-1 siRNA then exposed to 24 h hypoxia (1% O_2) with or without a CD47-blocking antibody. Data represent three independent experiments. Asterisk (*) indicates statistically significant difference ($P < 0.05$) compared with hypoxia control alone. Hash (#) indicates statistically significant difference ($P < 0.05$) compared with hypoxia alone. (*G*) Wild-type and TSP1 null pulmonary microvascular endothelial cells harvested from 10-week-old male animals were grown to 80% confluence, treated with normoxia or hypoxia (1% O_2) ± TSP1 (2.2 or 22 nmol/L) as indicated for 24 h, cell lysate prepared and western blot analysis for Cav-1 expression performed. A representative blot and accompanying densitometry from three separate experiments are presented. Quantification of densitometric analysis of the mean ratio of Cav-1 to α-tubulin. Asterisk (*) indicates statistically significant difference ($P < 0.05$) from normoxic untreated. Hash (#) indicates statistically significant difference ($P < 0.05$) from normoxic wild-type + 22 nmol/L TSP1 and hypoxic wild-type. (*H*) Western blot analysis for phospho-Cav-1^{Tyr14} expression in normoxic hPAEC treated with the indicated amounts of TSP1 (2.2 nmol/L) ± a CD47 antibody (B6H12, 1 μg/mL) for 30 m. Quantification of densitometric analysis of mean ratio p-Cav-1 to total Cav-1 of three separate experiments. Asterisk (*) indicates statistically significant difference ($P < 0.05$) from untreated and antibody alone. Hash (#) indicates statistically significant difference ($P < 0.05$) from TSP1 treated.

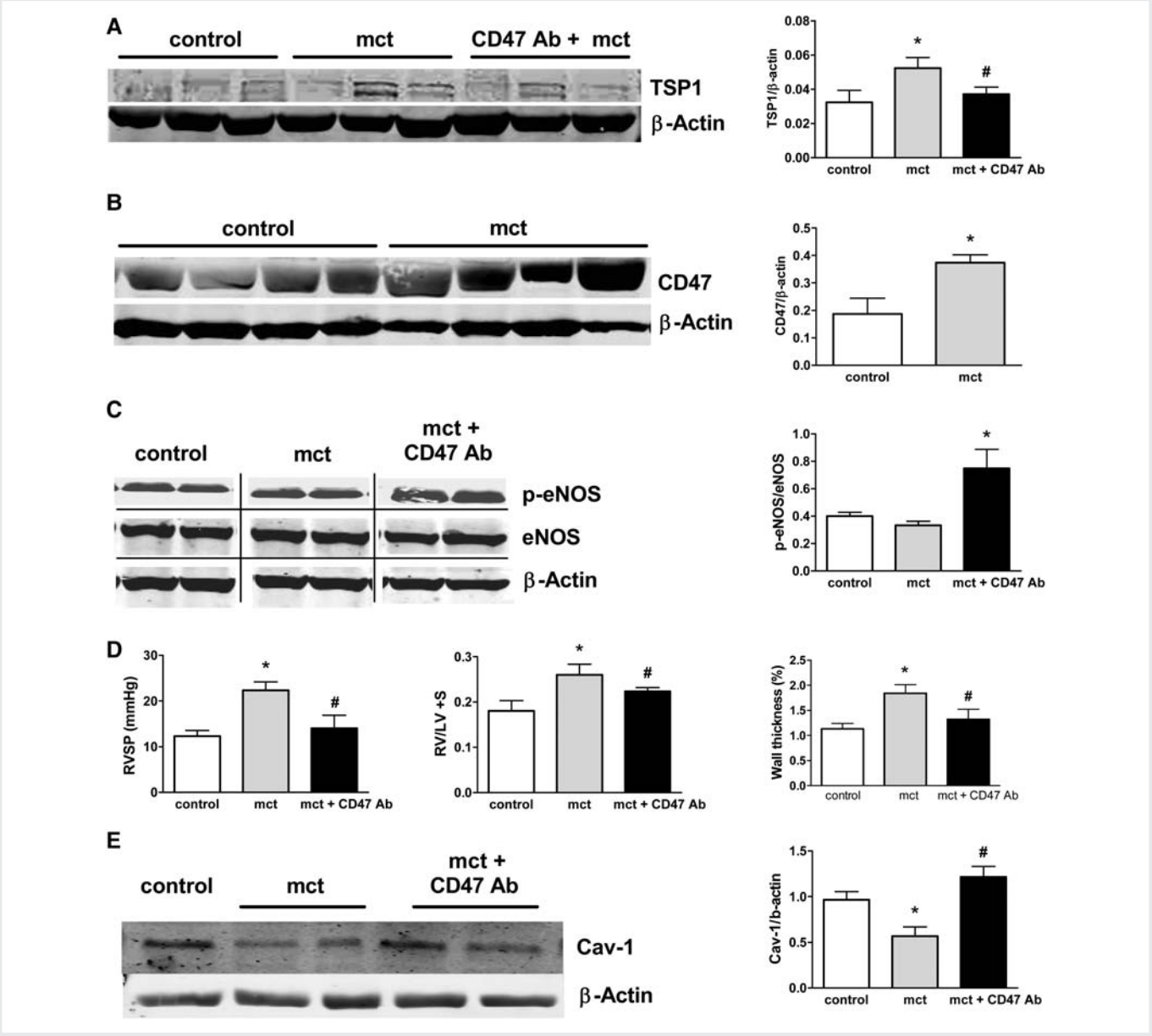

Figure 6 Blockade of CD47 activation upregulates Cav-1 and prevents experimental PAH. Age-matched male Sprague Dawley rats were treated with monocrotaline (mct, 50 mg/kg) ± a CD47-blocking antibody (clone OX101, 1 μg/gram body weight on day 1 and day 14 via i.p. injection). Animals were euthanized after 4 weeks. Lung lysates were prepared and proteins separated by SDS–PAGE electrophoresis. Blots were probed with a monoclonal antibody to (*A*) TSP1, (*B*) CD47, or (*C*) p-eNOS. Expression was quantified by densitometry and is presented as the mean ± SD. Densitometry results are from four animals in each group. (*A*) Asterisk (*) indicates statistically significant difference ($P < 0.05$) mct compared with control; Hash (#) indicates statistically significant difference ($P < 0.05$) mct compared with mct + CD47 antibody (Ab). (*B*) Asterisk (*) indicates statistically significant difference ($P < 0.05$) mct compared with control. (*C*) Asterisk (*) indicates statistically significant difference ($P < 0.05$) control compared with mct + CD47 antibody (Ab). (*D*) Age-matched male Sprague Dawley rats were treated with monocrotaline (mct) ± CD47 monoclonal antibody (Ab) (clone OX101, 1 μg/gram body weight) and right ventricular systolic pressure and RV/LV + S ratio (Fulton Index) measured at 4 weeks. Quantification of pulmonary arteriole wall thickness was performed by a blinded reviewer from tissue section images using an image analysis programme (Metamorph) with percent wall thickness defined as the wall thickness normalized to the vessel diameter and was specifically calculated by the following formula: wall thickness (%) = area external − area internal/area external × 100, where area external and area internal are the areas bounded by external elastic lamina and the lumen, respectively. Normalization was performed to account for increases in vessels size and wall thickness as a function of vessel diameter. Results are the mean ± SD of four animals in each group. Asterisk (*) indicates statistically significant difference ($P < 0.05$) mct compared with control. Hash (#) indicates statistically significant difference ($P < 0.05$) mct compared with mct + CD47 antibody (Ab). (*E*) Representative western blot of rat lung lysate from treated animals probed for Cav-1 and β-actin. Expression was quantified by densitometry presented as the mean ± SD from four animals in each group. Asterisk (*) indicates statistically significant difference ($P < 0.05$) control compared with mct. Hash (#) indicates statistically significant difference ($P < 0.05$) mct compared with mct + CD47 antibody (Ab).

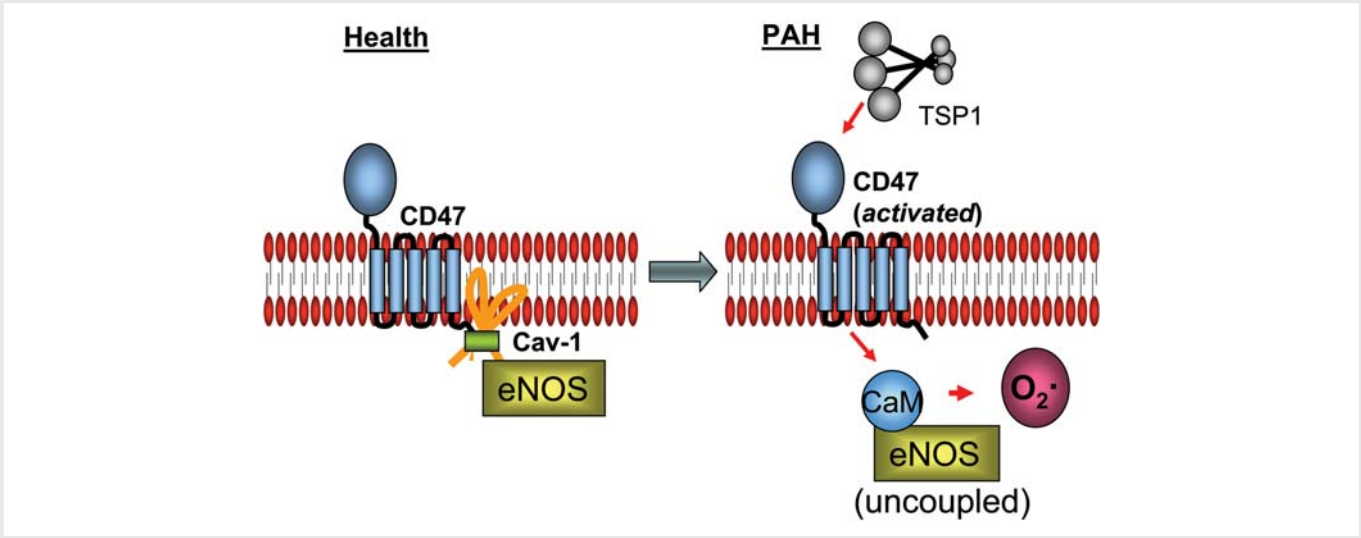

Figure 7 Activated CD47 promotes PAH through suppressing constitutive Cav-1 inhibition of eNOS. In health and under normoxic conditions, CD47 constitutively associates with Cav-1 on the cell membrane of pulmonary arterial endothelial cells. In hypoxia and PAH, the CD47 ligand TSP1 is upregulated. On binding with TSP1, the cell receptor CD47 is activated leading to disruption of the constitutive interaction between CD47 and Cav-1. This in turn leads to decreased Cav-1 and increased eNOS activity. Monomeric hyperactive eNOS then produces superoxide rather than NO resulting in tissue oxidation and nitration.

results are consistent with our report that in normoxic endothelial cells activated CD47-inhibited eNOS through limiting cellular calcium,[27] and inhibited NO-mediated[25] stimulation of soluble gaunylyl cyclase (sGC). It is possible that our current results in hypoxic null mice are, to some extent, mediated through these known functions of the TSP1-CD47 axis. This might also explain our finding that activated CD47 limited nitrite-mediated blood flow under hypoxic conditions.[48] It remains to be determined if, under hypoxia, activated CD47 directly inhibits NO-mediated activation of sGC.

CD47 and Cav-1 constitutively co-associate on pulmonary endothelial cells. TSP1 and hypoxia, through TSP1 induction, activate CD47 to disrupt this co-association and free eNOS from the inhibitory and protective effects of Cav-1 in these situations. TSP1, via CD47, also increased Cav-1 phosphorylation in pulmonary endothelial cells. It is not clear how TSP1-mediated disruption of Cav-1CD47 co-association alters Cav-1 levels or how TSP1 alters Cav-1 phosphorylation. However, Cav-1 is a target of activated CD47, and hence downstream in this process, since knock-down of Cav-1 mitigates ROS suppression from a CD47-blocking antibody in hypoxic pulmonary arterial endothelial cells.

Taken together, these data demonstrate that TSP1-mediated activation of CD47 promotes superoxide production from uncoupled eNOS by limiting the expression and hence activity of Cav-1 (*Figure 7*). These studies are important, in that they describe for the first time a role for activated CD47 in both experimental PAH and human disease, and identify Cav-1 as a target of CD47 signalling.

Supplementary material

Supplementary material is available at *Cardiovascular Research* online.

Conflict of interest: J.S.I. is chair of the SAB of Vasculox, Inc. (St Louis, MO, USA) and Radiation Control Technologies, Inc. (Rockville, MD, USA).

Funding

This work was supported by the National Cancer Institute (K22 CA128616 to J.S.I.); the National Heart Lung and Blood Institute (R01 HL-108954 to J.S.I.); the National Institutes of Health TPPG PO1HL103455 to J.S.I.; the American Heart Association (11BGIA7210001 to J.S.I.); the Institute for Transfusion Medicine and the Hemophilia Center of Western Pennsylvania (to J.S.I.), the National Institutes of Health (R01 HL-085134 and TPPG PO1HL103455 to P.M.B.); and the Ministerio de Ciencia e Innovacion (SAF2009-11113 to M.F.C.).

References

1. D'Alonzo GE, Barst RJ, Ayres SM, Bergofsky EH, Brundage BH, Detre KM *et al.* Survival in patients with primary pulmonary hypertension. Results from a national prospective registry. *Ann Intern Med* 1991;**115**:343–349.
2. Humbert M, Morrell NW, Archer SL, Stenmark KR, MacLean MR, Lang IM *et al.* Cellular and molecular pathobiology of pulmonary arterial hypertension. *J Am Coll Cardiol* 2004;**43**:13S–24S.
3. Mandegar M, Fung YC, Huang W, Remillard CV, Rubin LJ, Yuan JX. Cellular and molecular mechanisms of pulmonary vascular remodeling: role in the development of pulmonary hypertension. *Microvasc Res* 2004;**68**:75–103.
4. Simonneau G, Galie N, Rubin LJ, Langleben D, Seeger W, Domenighetti G *et al.* Clinical classification of pulmonary hypertension. *J Am Coll Cardiol* 2004;**43**: 5S–12S.
5. Gladwin MT, Sachdev V, Jison ML, Shizukuda Y, Plehn JF, Minter K *et al.* Pulmonary hypertension as a risk factor for death in patients with sickle cell disease. *N Engl J Med* 2004;**350**:886–895.
6. Khoo JP, Zhao L, Alp NJ, Bendall JK, Nicoli T, Rockett K *et al.* Pivotal role for endothelial tetrahydrobiopterin in pulmonary hypertension. *Circulation* 2005;**111**: 2126–2133.
7. Konduri GG, Ou J, Shi Y, Pritchard KA Jr. Decreased association of HSP90 impairs endothelial nitric oxide synthase in fetal lambs with persistent pulmonary hypertension. *Am J Physiol Heart Circ Physiol* 2003;**285**:H204–H211.
8. Lakshminrusimha S, Wiseman D, Black SM, Russell JA, Gugino SF, Oishi P *et al.* The role of nitric oxide synthase-derived reactive oxygen species in the altered relaxation of pulmonary arteries from lambs with increased pulmonary blood flow. *Am J Physiol Heart Circ Physiol* 2007;**293**:H1491–H1497.
9. Kobs RW, Chesler NC. The mechanobiology of pulmonary vascular remodeling in the congenital absence of eNOS. *Biomech Model Mechanobiol* 2006;**5**:217–225.

10. Fulton D, Gratton JP, Sessa WC. Post-translational control of endothelial nitric oxide synthase: why isn't calcium/calmodulin enough? *J Pharmacol Exp Ther* 2001;**299**: 818–824.
11. Shaul PW, Smart EJ, Robinson LJ, German Z, Yuhanna IS, Ying Y *et al*. Acylation targets emdothelial nitric-oxide synthase to plasmalemmal caveolae. *J Biol Chem* 1996;**271**:6518–6522.
12. Bauer PM, Yu J, Chen Y, Hickey R, Bernatchez PN, Looft-Wilson R *et al*. Endothelial-specific expression of caveolin-1 impairs microvascular permeability and angiogenesis. *Proc Natl Acad Sci USA* 2005;**102**:204–209.
13. Ju H, Zou R, Venema VJ, Venema RC. Direct interaction of endothelial nitric-oxide synthase and caveolin-1 inhibits synthase activity. *J Biol Chem* 1997;**272**: 18522–18525.
14. Sowa G, Pypaert M, Sessa WC. Distinction between signaling mechanisms in lipid rafts vs. caveolae.Proc Natl Acad Sci USA 2001;**98**:14072–14077.
15. Drab M, Verkade P, Elger M, Kasper M, Lohn M, Lauterbach B *et al*. Loss of caveolae, vascular dysfunction, and pulmonary defects in caveolin-1 gene-disrupted mice. *Science* 2001;**293**:2449–2452.
16. Razani B, Combs TP, Wang XB, Frank PG, Park DS, Russell RG *et al*. Caveolin-1-deficient mice are lean, resistant to diet-induced obesity, and show hypertriglyceridemia with adipocyte abnormalities. *J Biol Chem* 2002;**277**:8635–8647.
17. Zhao YY, Liu Y, Stan RV, Fan L, Gu Y, Dalton N *et al*. Defects in caveolin-1 cause dilated cardiomyopathy and pulmonary hypertension in knockout mice. *Proc Natl Acad Sci USA* 2002;**99**:11375–11380.
18. Murata T, Lin MI, Huang Y, Yu J, Bauer PM, Giordano FJ *et al*. Reexpression of caveolin-1 in endothelium rescues the vascular, cardiac, and pulmonary defects in global caveolin-1 knockout mice. *J Exp Med* 2007;**204**:2373–2382.
19. Wunderlich C, Schmeisser A, Heerwagen C, Ebner B, Schober K, Braun-Dullaeus RC *et al*. Chronic NOS inhibition prevents adverse lung remodeling and pulmonary arterial hypertension in caveolin-1 knockout mice. *Pulm Pharmacol Ther* 2008;**21**:507–515.
20. Zhao YY, Zhao YD, Mirza MK, Huang JH, Potula HH, Vogel SM *et al*. Persistent eNOS activation secondary to caveolin-1 deficiency induces pulmonary hypertension in mice and humans through PKG nitration. *J Clin Invest* 2009;**119**:2009–2018.
21. Achcar RO, Demura Y, Rai PR, Taraseviciene-Stewart L, Kasper M, Voelkel NF *et al*. Loss of caveolin and heme oxygenase expression in severe pulmonary hypertension. *Chest* 2006;**129**:696–705.
22. Patel HH, Zhang S, Murray F, Suda RY, Head BP, Yokoyama U *et al*. Increased smooth muscle cell expression of caveolin-1 and caveolae contribute to the pathophysiology of idiopathic pulmonary arterial hypertension. *FASEB J* 2007;**21**:2970–2979.
23. Isenberg JS, Hyodo F, Matsumoto K, Romeo MJ, Abu-Asab M, Tsokos M *et al*. Thrombospondin-1 limits ischemic tissue survival by inhibiting nitric oxide-mediated vascular smooth muscle relaxation. *Blood* 2007;**109**:1945–1952.
24. Isenberg JS, Calzada MJ, Zhou L, Guo N, Lawler J, Wang XQ *et al*. Endogenous thrombospondin-1 is not necessary for proliferation but is permissive for vascular smooth muscle cell responses to platelet-derived growth factor. *Matrix Biol* 2005; **24**:110–123.
25. Isenberg JS, Ridnour LA, Perruccio EM, Espey MG, Wink DA, Roberts DD. Thrombospondin-1 inhibits endothelial cell responses to nitric oxide in a cGMP-dependent manner. *Proc Natl Acad Sci USA* 2005;**102**:13141–13146.
26. Isenberg JS, Ridnour LA, Dimitry J, Frazier WA, Wink DA, Roberts DD. CD47 is necessary for inhibition of nitric oxide-stimulated vascular cell responses by thrombospondin-1. *J Biol Chem* 2006;**281**:26069–26080.
27. Bauer EM, Qin Y, Miller TW, Bandle RW, Csanyi G, Pagano PJ *et al*. Thrombospondin-1 supports blood pressure by limiting eNOS activation and endothelial-dependent vasorelaxation. *Cardiovasc Res* 2010;**88**:471–481.
28. Zuckerbraun BS, Chin BY, Wegiel B, Billiar TR, Czsimadia E, Rao J *et al*. Carbon monoxide reverses established pulmonary hypertension. *J Exp Med* 2006;**203**:2109–2119.
29. Stenmark KR, Meyrick B, Galie N, Mooi WJ, McMurtry IF. Animal models of pulmonary arterial hypertension: the hope for etiological discovery and pharmacological cure. *Am J Physiol Lung Cell Mol Physiol* 2009;**297**:L1013–L1032.
30. Bonnet S, Michelakis ED, Porter CJ, Andrade-Navarro MA, Thebaud B, Haromy A *et al*. An abnormal mitochondrial-hypoxia inducible factor-1alpha-Kv channel pathway disrupts oxygen sensing and triggers pulmonary arterial hypertension in fawn hooded rats: similarities to human pulmonary arterial hypertension. *Circulation* 2006;**113**:2630–2641.
31. Caruso P, MacLean MR, Khanin R, McClure J, Soon E, Southgate M *et al*. Dynamic changes in lung microRNA profiles during the development of pulmonary hypertension due to chronic hypoxia and monocrotaline. *Arterioscler Thromb Vasc Biol* 2010;**30**: 716–723.
32. Antezana AM, Antezana G, Aparicio O, Noriega I, Velarde FL, Richalet JP. Pulmonary hypertension in high-altitude chronic hypoxia: response to nifedipine. *Eur Respir J* 1998;**12**:1181–1185.
33. Lawler J, Sunday M, Thibert V, Duquette M, George EL, Rayburn H *et al*. Thrombospondin-1 is required for normal murine pulmonary homeostasis and its absence causes pneumonia. *J Clin Invest* 1998;**101**:982–992.
34. Burt C, Pepke-Zaba J, Falter F. Pulmonary arterial hypertension. *Curr Vasc Pharmacol* 2010;**8**:412–420.
35. Fulton D, Gratton JP, McCabe TJ, Fontana J, Fujio Y, Walsh K *et al*. Regulation of endothelium-derived nitric oxide production by the protein kinase Akt. *Nature* 1999;**399**:597–601.
36. Sessa WC. eNOS at a glance. *J Cell Sci* 2004;**117**:2427–2429.
37. Li H, Wallerath T, Munzel T, Forstermann U. Regulation of endothelial-type NO synthase expression in pathophysiology and in response to drugs. *Nitric Oxide* 2002;**7**: 149–164.
38. Isenberg JS, Annis DS, Pendrak ML, Ptaszynska M, Frazier WA, Mosher DF *et al*. Differential interactions of thrombospondin-1, -2, and -4 with CD47 and effects on cGMP signaling and ischemic injury responses. *J Biol Chem* 2009;**284**:1116–1125.
39. Lim EJ, Smart EJ, Toborek M, Hennig B. The role of caveolin-1 in PCB77-induced eNOS phosphorylation in human-derived endothelial cells. *Am J Physiol Heart Circ Physiol* 2007;**293**:H3340–3347.
40. Zheng C, Wang L, Li R, Ma B, Tu L, Xu X *et al*. Gene delivery of cytochrome p450 epoxygenase ameliorates monocrotaline-induced pulmonary artery hypertension in rats. *Am J Respir Cell Mol Biol* 2010;**43**:740–749.
41. Huang J, Kaminski PM, Edwards JG, Yeh A, Wolin MS, Frishman WH *et al*. Pyrrolidine dithiocarbamate restores endothelial cell membrane integrity and attenuates monocrotaline-induced pulmonary artery hypertension. *Am J Physiol Lung Cell Mol Physiol* 2008;**294**:L1250–L1259.
42. Redout EM, Wagner MJ, Zuidwijk MJ, Boer C, Musters RJ, van Hardeveld C *et al*. Right-ventricular failure is associated with increased mitochondrial complex II activity and production of reactive oxygen species. *Cardiovasc Res* 2007;**75**:770–781.
43. Maxhimer JB, Shih HB, Isenberg JS, Miller TW, Roberts DD. Thrombospondin-1/ CD47 blockade following ischemia-reperfusion injury is tissue protective. *Plast Reconstr Surg* 2009;**124**:1880–1889.
44. Lobysheva I, Rath G, Sekkali B, Bouzin C, Feron O, Gallez B *et al*. Moderate caveolin-1 downregulation prevents NADPH oxidase-dependent endothelial nitric oxide synthase uncoupling by angiotensin II in endothelial cells. *Arterioscler Thromb Vasc Biol* 2011;**31**:2098–2105.
45. Taubert D, Berkels R, Grosser N, Schroder H, Grundemann D, Schomig E. Aspirin induces nitric oxide release from vascular endothelium: a novel mechanism of action. *Br J Pharmacol* 2004;**143**:159–165.
46. Fleming I, Busse R. Signal transduction of eNOS activation. *Cardiovasc Res* 1999;**43**: 532–541.
47. Dimmeler S, Dernbach E, Zeiher AM. Phosphorylation of the endothelial nitric oxide synthase at ser-1177 is required for VEGF-induced endothelial cell migration. *FEBS Lett* 2000;**477**:258–262.
48. Isenberg JS, Shiva S, Gladwin M. Thrombospondin-1-CD47 blockade and exogenous nitrite enhance ischemic tissue survival, blood flow and angiogenesis via coupled NO-cGMP pathway activation. *Nitric Oxide* 2009;**21**:52–62.